diabetes®
American Diabetes Association®

IL-6 Trans-Signaling Is Increased in Diabetes, Impacted by Glucolipotoxicity, and Associated With Liver Stiffness and Fibrosis in Fatty Liver Disease

Aysim Gunes, Clémence Schmitt, Laurent Bilodeau, Catherine Huet, Assia Belblidia, Cindy Baldwin, Jeanne-Marie Giard, Laurent Biertho, Annie Lafortune, Christian Yves Couture, Angela Cheung, Bich N. Nguyen Eithan Galun, Chantal Bémeur, Marc Bilodeau, Mathieu Laplante, An Tang, May Faraj, and Jennifer L. Estall

Diabetes 2023;72(12):1820–1834 | https://doi.org/10.2337/db23-0171

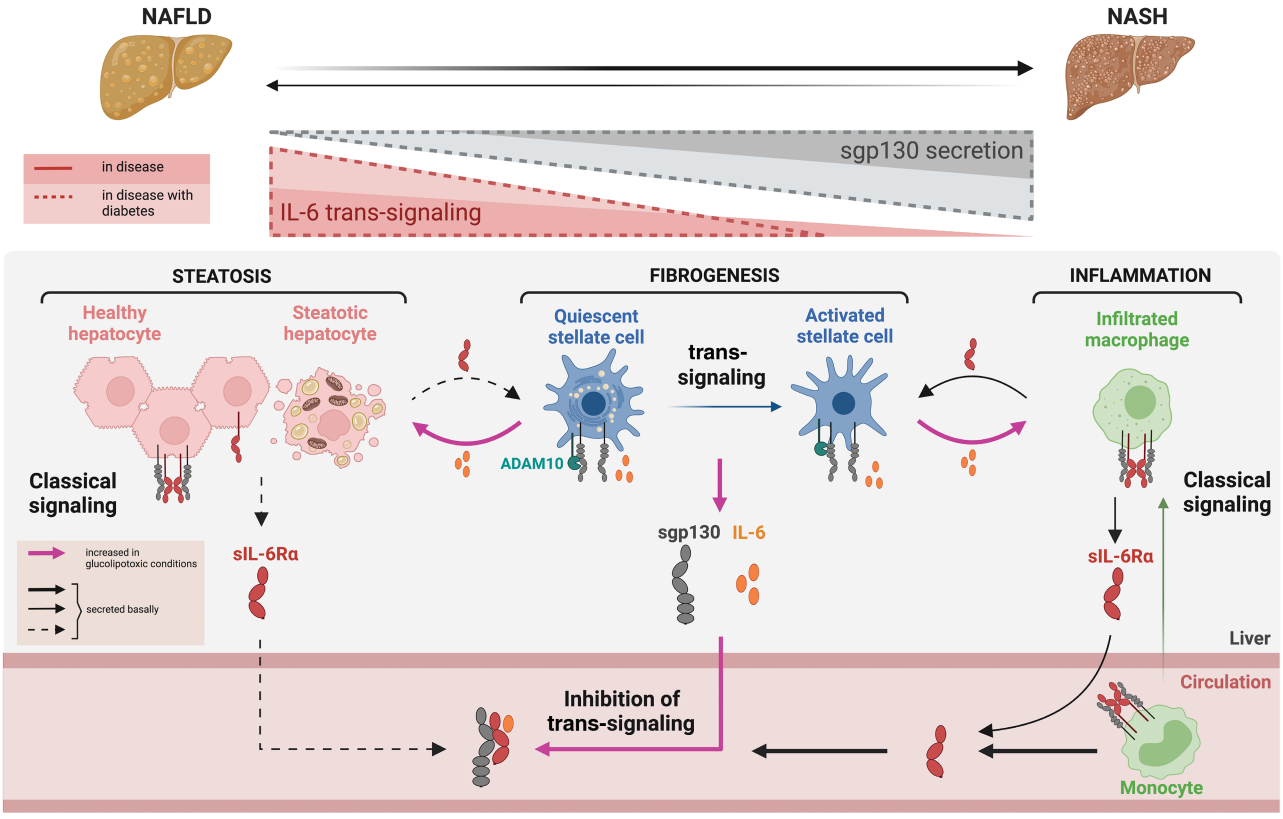

NAFLD, nonalcoholic fatty liver disease; NASH, nonalcoholic steatosis.

PATHOPHYSIOLOGY

IL-6 Trans-Signaling Is Increased in Diabetes, Impacted by Glucolipotoxicity, and Associated With Liver Stiffness and Fibrosis in Fatty Liver Disease

Aysim Gunes,[1,2,3] Clémence Schmitt,[1,4] Laurent Bilodeau,[5] Catherine Huet,[5] Assia Belblidia,[5] Cindy Baldwin,[1] Jeanne-Marie Giard,[6] Laurent Biertho,[7,8] Annie Lafortune,[7,8] Christian Yves Couture,[7,9] Angela Cheung,[10] Bich N. Nguyen[11] Eithan Galun,[12] Chantal Bémeur,[13,14] Marc Bilodeau,[6] Mathieu Laplante,[3,7] An Tang,[5] May Faraj,[1,2,3,13] and Jennifer L. Estall[1,2,3,4]

Diabetes 2023;72:1820–1834 | https://doi.org/10.2337/db23-0171

Many people living with diabetes also have nonalcoholic fatty liver disease (NAFLD). Interleukin-6 (IL-6) is involved in both diseases, interacting with both membrane-bound (classical) and circulating (trans-signaling) soluble receptors. We investigated whether secretion of IL-6 trans-signaling coreceptors are altered in NAFLD by diabetes and whether this might associate with the severity of fatty liver disease. Secretion patterns were investigated with use of human hepatocyte, stellate, and monocyte cell lines. Associations with liver pathology were investigated in two patient cohorts: *1*) biopsy-confirmed steatohepatitis and *2*) class 3 obesity. We found that exposure of stellate cells to high glucose and palmitate increased IL-6 and soluble gp130 (sgp130) secretion. In line with this, plasma sgp130 in both patient cohorts positively correlated with HbA_{1c}, and subjects with diabetes had higher circulating levels of IL-6 and trans-signaling coreceptors. Plasma sgp130 strongly correlated with liver stiffness and was significantly increased in subjects with F4 fibrosis stage. Monocyte activation was associated with reduced sIL-6R secretion. These data suggest that hyperglycemia and hyperlipidemia can directly impact IL-6 trans-signaling and that this may be linked to enhanced severity of NAFLD in patients with concomitant diabetes.

ARTICLE HIGHLIGHTS

- IL-6 and its circulating coreceptor sgp130 are increased in people with fatty liver disease and steatohepatitis.
- High glucose and lipids stimulated IL-6 and sgp130 secretion from hepatic stellate cells.
- sgp130 levels correlated with HbA_{1c}, and diabetes concurrent with steatohepatitis further increased circulating levels of all IL-6 trans-signaling mediators.
- Circulating sgp130 positively correlated with liver stiffness and hepatic fibrosis.
- Metabolic stress to liver associated with fatty liver disease might shift the balance of IL-6 classical versus trans-signaling, promoting liver fibrosis that is accelerated by diabetes.

[1]Institut de recherches cliniques de Montréal (IRCM), Montreal, Quebec, Canada
[2]Division of Experimental Medicine, McGill University, Montreal, Quebec, Canada
[3]Montreal Diabetes Research Centre, Montreal, Quebec, Canada
[4]Programmes de biologie moléculaire, Faculté de médecine, Université de Montréal, Montreal, Quebec, Canada
[5]Département de radiologie, Centre hospitalier de l'Université de Montréal (CHUM), Montreal, Quebec, Canada
[6]Liver Unit, Centre hospitalier de l'Université de Montréal (CHUM), Département de médecine, Université de Montréal, Montreal, Quebec, Canada
[7]Centre de recherche de l'Institut universitaire de cardiologie et de pneumologie de Québec, Université Laval, Quebec City, Quebec, Canada
[8]Département de chirurgie, Faculté de médecine, Université Laval, Quebec City, Quebec, Canada
[9]Département de biologie moléculaire, biochimie médicale et pathologie, Université Laval, Quebec City, Quebec, Canada
[10]Gastroenterology and Hepatology, Department of Medicine, The Ottawa Hospital, Ottawa, Ontario, Canada
[11]Département de pathologie et biologie cellulaire, Université de Montréal, Montreal, Quebec, Canada
[12]Goldyne Savad Institute of Gene Therapy, Hadassah Hebrew University Hospital, Jerusalem, Israel
[13]Département de nutrition, Université de Montréal, Montreal, Quebec, Canada
[14]Labo HépatoNeuro, Centre de recherche du CHUM, Montreal, Quebec, Canada

Corresponding author: Jennifer L. Estall, jennifer.estall@ircm.qc.ca

Received 28 February 2023 and accepted 31 August 2023

This article contains supplementary material online at https://doi.org/10.2337/figshare.24114459.

Nonalcoholic fatty liver disease (NAFLD) is a multistep, progressive disorder beginning with simple steatosis that can evolve to nonalcoholic steatohepatitis (NASH), characterized by hepatocellular ballooning, lobular inflammation, and fibrosis. NAFLD prevalence is rapidly increasing worldwide, currently affecting 25% of the population (1). The biological and physiological signals corresponding to and mediating the transition from simple steatosis to the more advanced and pathogenic stages of NASH are not well understood. NAFLD is closely associated with obesity and diets high in fat and sugar (2). NAFLD stemming from metabolic disease, recently reclassified as metabolically associated steatotic liver disease (MASLD) (3), is often diagnosed in conjunction with diabetes. Upward of 70–80% of people with diabetes also have MASLD, and conversely, MASLD increases one's risk of developing diabetes by two- to threefold (4). Whether or how one disease impacts the other is unclear.

Liver inflammation plays a key role in the transition of simple steatosis to steatohepatitis. Interleukin-6 (IL-6) is an inflammatory cytokine closely associated with metabolic disease (5,6), has both pro- and anti-inflammatory properties, and may play a role in the progression of NAFLD to NASH (7,8). IL-6 signaling involves activation of either a membrane-bound receptor (classical) or formation of a signaling complex with a soluble (s)IL-6 receptor found in circulation (trans-signaling). Both types of signaling require the ligand/receptor complex to bind a coreceptor, glycoprotein 130 (gp130), on the surface of cells. Circulating IL-6R (sIL-6R), shed from receptor-expressing cells, can dock gp130 on distant cells, allowing IL-6 trans-signaling in tissues that do not express the IL-6R. A soluble, secreted form of the coreceptor (sgp130) also circulates and can inhibit trans-signaling by sequestering the IL-6/sIL-6R complex (9). Based on expression patterns, hepatocytes and hepatic stellate cells may be a rich source of sIL-6R and sgp130, respectively, suggesting the liver as a potential major player in IL-6 trans-signaling (10,11). There is evidence linking increased IL-6 trans-signaling to other metabolic diseases including diabetes (12–14), as well as to alcohol- and infection-induced chronic liver disease (11).

While classical IL-6 signaling is known to have close links to NAFLD and metabolic disease, associations between IL-6 trans-signaling and NAFLD/NASH have not been evaluated. In this study, we investigated whether the liver could be a significant source of these circulating coreceptors and whether their levels relate to liver pathology associated with diabetes in two human cohorts with NAFLD. We also investigated whether metabolic stress influences the secretion of IL-6 trans-signaling mediators from liver cell types.

RESEARCH DESIGN AND METHODS

Human Cell Lines

HepG2 cells were cultured in DMEM (1.0 g/L glucose) with 10% FBS, streptomycin/penicillin, and 1% nonessential amino acids. LX-2 cells were cultured in DMEM (4.5 g/L glucose) with 5% FBS, streptomycin/penicillin, and 1 mmol/L sodium pyruvate. THP-1 cells were cultured in RPMI medium (2.0 g/L glucose) with 10% FBS, streptomycin/penicillin, and 1 mmol/L sodium pyruvate. Cell lines were plated at 250,000 cells/mL. LX-2 cells were activated with 5 ng/mL transforming growth factor-β for 48 h (0.5% FBS) followed by 24 h recovery (5% FBS). THP-1 cells were activated with 100 nmol/L propidium monoazide (PMA) for 48 h. For glucolipotoxic challenge, cells were starved overnight in media with 0.5% FBS prior to treatment in similar media with control (BSA vehicle) or additional 25 mmol/L D-glucose and 250 μmol/L sodium palmitate (conjugated to BSA, 1:6) for 18 h.

Conditioned media were collected and cells harvested for mRNA (Trizol) or protein (radioimmunoprecipitation assay [RIPA]). For inhibitor studies, LX-2 cells were treated with vehicle (DMSO), 3 μmol/L GI254023X (GI) (no. AOB3611, ADAM10 inhibitor; AOBIOUS), or 3 μmol/L GW280264X (GW) (AOB3632, ADAM10/17 inhibitor; AOBIOUS) 30 min before glucose/palmitate challenge. For ADAM10 Western blot, RIPA buffer was supplemented with 5 μmol/L GI254023X for prevention of autocatalytic degradation.

Quantification of Media and Serum Cytokines

IL-6, sIL-6R, and sgp130 were measured in conditioned media or plasma with ELISA, according to instructions (D6050, DR600, and DGP00, Human Quantikine ELISA kits; R&D Systems). Levels of secreted proteins were normalized to total cellular protein.

RNA and Protein Quantification

DNAse-treated RNA (1 μg) was reversed transcribed (High-Capacity cDNA Reverse Transcription Kit; Applied Biosystems) and RT-qPCR performed (G892, BlasTaq qPCR MasterMix; Applied Biological Materials) with use of primers: *GP130* (forward, 5′-GCAACATTCTTACATTCGGACAG-3′; reverse, 5′-CTCGTTCACAATGCAACTCAAA-3′), *IL-6R* (forward, 5′-CCTCTGCATTGCCATTGTTC-3′; reverse, 5′-ATGCTTGTCTTGCCTTCCT-3′), *IL-6* (forward, 5′-CCCTGACCCAACCACAAA-3′; reverse, 5′-GGACTGCAGGAACTCCTTAAA-3′), *ADAM10* (forward, 5′-CCAACAAGGACATGAATT-3′; reverse, 5′-TGTTCCCAGTGCTGGTTTAG-3′), *ADAM17* (forward, 5′-CGTGGTGGTGGATGGTAAA-3′; reverse, 5′-ATGTGGGCTAGAACCCTAGA-3′), and *RPLP0* (forward, 5′-CGAAATGTTTCATTGTGGGAG-3′; reverse, 5′-CATTCCCCCGGATATGAGGCAGCA-3′). Relative mRNA expressed as $2^{-\Delta Ct}$ were normalized to *RPLP0*.

Proteins solubilized in RIPA were resolved with SDS-PAGE, transferred to nitrocellulose, and probed with anti-ADAM10 (14194; Cell Signaling Technology) or anti–β-ACTIN (A5441; Sigma-Aldrich). ChemiDoc (Bio-Rad Laboratories) and Image Lab software were used to capture and quantify signals.

Patients With NASH

Plasma samples, histological liver scoring, and MRI/magnetic resonance elastography (MRE) data were obtained

from 50 patients with NASH (28 women, 22 men) previously recruited from a registry of patients with NASH (study initiated in 2016 with ethics approval at Centre hospitalier de l'Université de Montréal, institutional review board no. 15.147). All selected participants in the current study (institutional review board no. 17.031) provided written informed consent allowing preservation and use of their plasma samples and data.

Subjects were aged 18 years and older, diagnosed with NASH (biopsy confirmed), and able to undergo MRI without contrast agent. Subjects were excluded on the basis of alcohol consumption (>10 drinks/week for women and >15 for men) or if they had liver disease other than NASH, were taking medications associated with steatosis (e.g., amiodarone, valproate, tamoxifen, methotrexate, or corticosteroids), were physically unable to fit in the MRI, had contraindications to MRI, or were pregnant or wished to be pregnant during that year. One patient without steatosis and 10 with previous history of hepatocellular carcinoma were excluded. Proton density fat fraction, liver volume (voxels, cm^3), and liver stiffness (Pa) were measured as quantitative predictors of liver fat, volume, and fibrosis, respectively. Average proton density fat fraction values for the entire liver volume were obtained with use of the LiverLab package (version VE11C, MAGNETOM Aera; Siemens Healthineers). Liver stiffness by MRE was measured as previously described (15). Repeatability, reproducibility, and accuracy of MRE in NAFLD were previously reported (16,17). Fasting plasma samples were collected on the day of

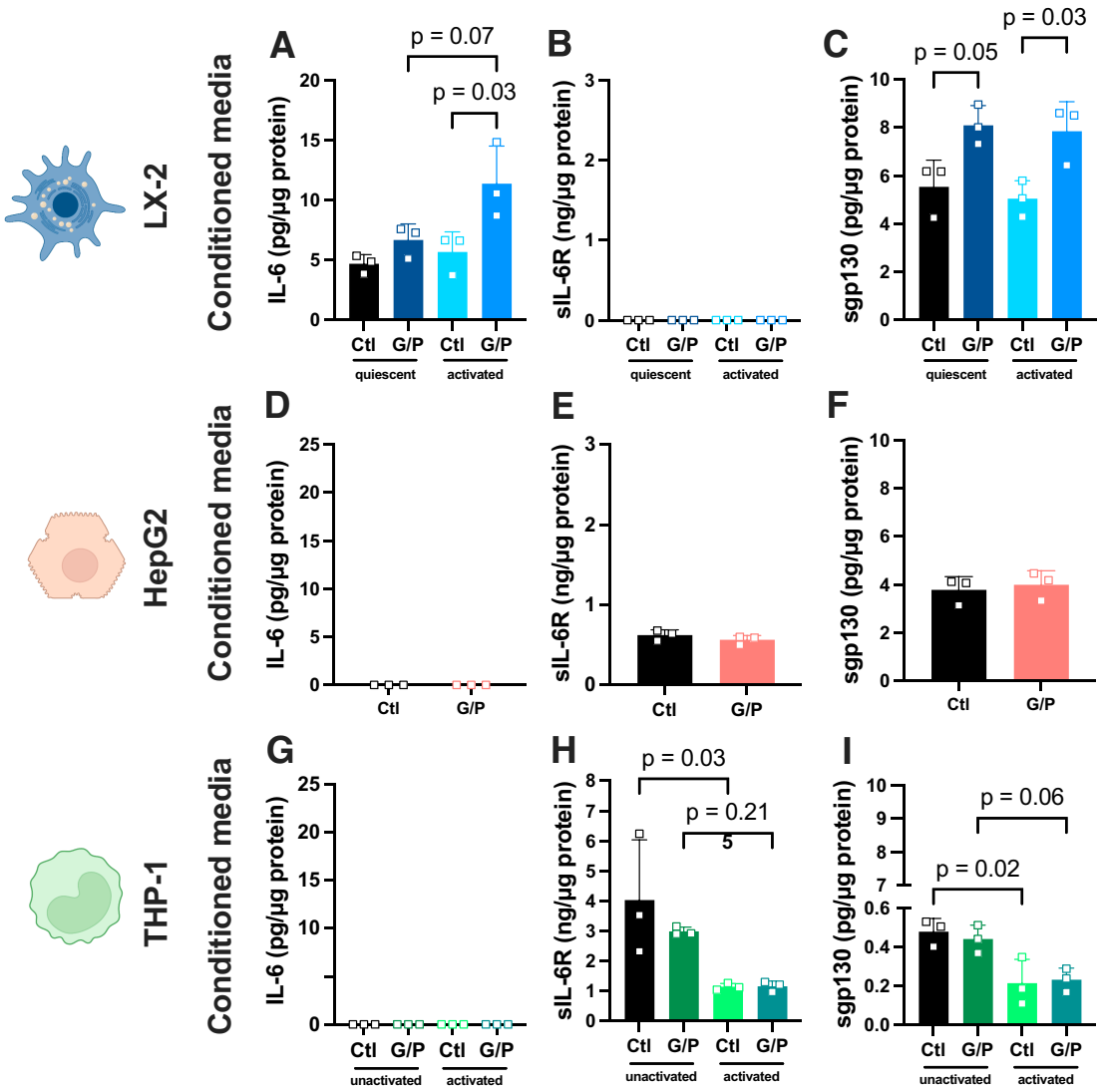

Figure 1—Secretion of IL-6 signaling mediators is influenced in hepatic stellate cells by glucolipotoxicity. Levels of IL-6 (*A*, *D*, and *G*), sIL-6R (*B*, *E*, and *H*), and sgp130 (*C*, *F*, and *I*) in conditioned media from quiescent and activated LX-2 and HepG2 cells, and unactivated and activated THP-1 cells. Cells were treated with high glucose and palmitate (G/P) or BSA vehicle (control [Ctl]) for 18 h, and secreted protein levels normalized to total cell protein. Analyses were performed with one-way ANOVA with multiple comparisons. Data shown are a representative experiment of three independent biological replicates, with three technical replicates for each.

the MRI/MRE and stored at −80°C. Fibrosis stages, activity scores, and steatosis grades were determined by a pathologist according to the NASH Clinical Research Network histological scoring system (18) on liver biopsies taken 6–12 months prior to MRI/MRE.

Patients With Class 3 Obesity

Plasma samples and matching liver biopsies were obtained from Institut universitaire de cardiologie et de pneumologie de Québec (IUCPQ) Biobank, Université Laval, in compliance with IRB-approved management policies initiated in 2002 and still ongoing. Liver biopsy samples were collected at the time of bariatric surgery with ethics approval (IRB no. 1142). Adult men and women (18 years and older) were selected from the registry of 4,781 patients. Exclusion criteria were alcohol consumption (>10 drinks/week for women and >15 for men) or liver disease other than NASH (e.g., autoimmune hepatitis, Wilson disease, hemochromatosis, hepatitis B virus, hepatitis C virus, human immunodeficiency viruses). Our retrospective analysis included a subpopulation of 245 subjects who had both blood samples and histological scoring data available. Group selection prioritized equal representation of sex (123 men, 122 women) and fibrosis stage (F0–F4).

Random blood samples were collected on the night before surgery and stored at −80°C until analysis. Sampling procedure and position were standardized among surgeons. Liver samples were obtained by incisional biopsy of the left lobe and not cauterized. Grading and staging of histological liver sections were performed according to the methodology of Brunt (19) by pathologists blinded to study objectives. The algorithm of Bedossa et al. (20) was used to diagnose NASH, with use of liver biopsy scores for hepatocellular ballooning stage (0–2), lobular inflammation (0–2), steatosis grade (G0–G3), activity score (A0–A4), and fibrosis stage (F0–F4). Since participants in both cohorts were diagnosed prior to 2023 guidelines for MASLD, not all precisely fit this new designation. Thus, we have chosen to use the older classifications of NAFLD and NASH herein for accuracy.

Statistics

Data are presented as mean ± SD for continuous variables and number of subjects (n) and percentage (%) for categorical variables. Normality was evaluated with Kolmogrov-Smirnov test. When normality failed, data were log transformed ($\log_{10}$). Outliers and influencers were identified with SPSS. One subject (NASH cohort) was a strong influencer for plasma IL-6 and sIL-6R and excluded from all analyses. Data were analyzed with unpaired t test, one-way ANOVA, and Pearson correlation as indicated. Sensitivity analysis was performed with Mann-Whitney U test for intergroup differences. For categorical variables, χ^2 test was used for count >5; otherwise, Fisher exact test was used. Since the number of these covariates should not be >10% of patient number, stepwise forward regression analysis (liver fat fraction, volume, and stiffness) and univariate analysis (steatosis grade, activity score, fibrosis stage) for the NASH cohort were adjusted with two models (model 1, age, sex, BMI, and diabetes; model 2, age, sex, BMI, and metformin). Diabetes and metformin were classified in different models due to their strong association ($P < 0.001$). For the morbid obesity cohort, univariate analysis (steatosis grade, activity score, hepatocellular ballooning, lobular, portal inflammation, and fibrosis stage) was adjusted with age, sex, BMI, diabetes, and metformin in one model. Data were analyzed with IBM SPSS (version 27) and GraphPad Prism (version 8), and significance was set at $P < 0.05$.

Data and Resource Availability

Data, analytical methods, and study materials are available on request.

RESULTS

Hepatic Stellate Cells Express and Secrete sgp130 in Response to Glucolipotoxic Stress

As NASH progresses, the proportion of hepatocytes in liver decreases, whereas hepatic stellate cells and macrophages increase with each fibrosis stage (21). Since inflammation is an important component of the simple steatosis–to–NASH transition, we hypothesized that IL-6 trans-signaling may be

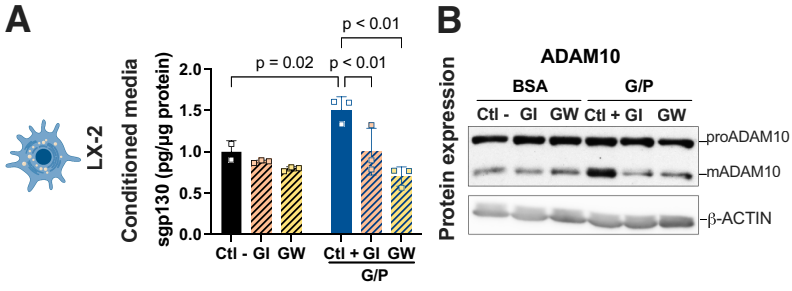

Figure 2—Inhibition of the ADAM10 protease blocks glucolipotoxicity-induced sgp130 secretion. Cells were treated with either GI or GW inhibitor 30 min prior to high glucose and palmitate (G/P) or BSA vehicle (control [Ctl]) for 18 h. *A*: Sgp130 secretion was assessed and normalized to total protein content. *B*: proADAM10 and mADAM10 protein levels were visualized with Western blot using β-ACTIN as loading control. Analyses were performed with one-way ANOVA with multiple comparisons. Data shown is one representative experiment of three independent biological replicates, each with two to three technical replicates.

Table 1—Anthropometric, metabolic, and clinical characteristics of patients with NASH

	Total (*n* = 38)	Women (*n* = 24)	Men (*n* = 14)	*P*
Baseline characteristics				
Age (years)	50.8 ± 13.1	51.4 ± 12.6	49.7 ± 14.4	0.712
Weight (kg)	91.1 ± 21.9	89.1 ± 23.0	94.5 ± 20.2	0.472
Height (cm)	169.5 ± 9.2	166.7 ± 9.3	174.3 ± 7.1	**0.012**
BMI (kg/m^2)	31.4 ± 5.6	31.8 ± 6.2	30.8 ± 4.5	0.695
Clinical parameters, *n* (%)				
Diabetes	17 (44.7)	12 (50.0)	5 (35.7)	0.393
Obesity	18 (47.4)	10 (41.7)	8 (57.1)	0.357
Hyperlipidemia	12 (31.6)	8 (33.3)	4 (28.6)	0.528
Hypertension	15 (39.5)	10 (41.7)	5 (35.7)	0.717
Medications, *n* (%)				
Metformin	14 (36.8)	11 (45.8)	3 (21.4)	0.132
Statins	10 (26.3)	7 (29.2)	3 (21.4)	0.451
Corticosteroids	1 (2.6)	1 (4.2)	0 (0.0)	0.632
Nifedipine	1 (2.6)	1 (4.2)	0 (0.0)	0.632
MRI/MRE data				
Liver fat fraction (%)	14.2 ± 9.0	13.0 ± 9.3	16.3 ± 8.4	0.283
Liver stiffness (Pa)	2,894.8 ± 1,297.4	2,714.6 ± 1,262.1	3,203.7 ± 1,345.4	0.113
Liver volume (cm^3)	2,084.0 ± 721.6	2,031.8 ± 754.1	2,173.4 ± 679.7	0.361
Fasting plasma parameters				
Hemoglobin (mg/dL)[a]	141.6 ± 12.9	138.4 ± 14.0	147.3 ± 8.2	**0.045**
Globulin (g/dL)[a]	6.7 ± 2.3	6.9 ± 2.4	6.2 ± 2.1	0.369
INR-PT[b]	0.9 ± 0.1	0.9 ± 0.1	0.9 ± 0.1	0.125
Platelet count (*10^9/L)[a]	218.2 ± 69.5	231.3 ± 77.2	195.0 ± 47.6	0.134
AST (U/L)[a]	33.0 ± 17.4	29.3 ± 13.9	39.6 ± 21.3	0.120
ALT (IU/L)[a]	55.1 ± 42.0	44.4 ± 22.2	73.8 ± 60.4	0.392
ALP (IU/L)[a]	70.3 ± 25.7	73.1 ± 26.7	65.2 ± 24.2	0.292
Total bilirubin (μmol/L)[a]	11.5 ± 6.1	11.1 ± 6.8	12.2 ± 4.7	0.066
GGT (units/L)[a]	56.6 ± 62.1	43.0 ± 44.0	80.7 ± 81.8	0.066
Albumin (g/L)[a]	44.5 ± 2.5	43.6 ± 2.2	46.2 ± 2.1	**0.002**
Glycemia (mmol/L)[b]	6.8 ± 3.0	6.9 ± 2.8	6.6 ± 3.4	0.607
HbA_{1c} (%)[b]	6.1 ± 1.1	6.1 ± 1.0	6.2 ± 1.4	0.781
Cholesterol (mmol/L)[b]	4.4 ± 1.1	4.7 ± 1.0	4.0 ± 1.0	0.059
HDL-c (mmol/L)[b]	1.1 ± 0.2	1.2 ± 0.3	1.0 ± 0.2	0.102
LDL-c (mmol/L)[c]	2.5 ± 0.9	2.8 ± 0.9	2.1 ± 0.8	**0.037**
Triglyceride (mmol/L)[b]	2.0 ± 1.3	1.8 ± 0.9	2.2 ± 1.7	0.443
CK-18 (units/L)	302.9 ± 255.3	246.5 ± 165.9	399.5 ± 347.7	0.341
Plasma components of the IL-6 pathway				
IL-6 (pg/mL)	6.1 ± 7.1	7.4 ± 8.4	3.9 ± 3.3	0.055
sIL-6R (ng/mL)	37.7 ± 11.2	38.5 ± 10.5	36.2 ± 12.8	0.397
sgp130 (ng/mL)	313.8 ± 56.8	313.1 ± 58.7	315.0 ± 55.6	0.864

Data are means ± SD for continuous data and sample size (*n*) and percent within the population (%) for categorical data. *P* values are comparisons between men and women, measured with unpaired *t* test for continuous data and χ^2 or Fisher exact test for categorical data. Bolded *P* values represent statistically significant differences. ALP, alkaline phosphatase; HDL-c, HDL cholesterol; LDL-c, LDL cholesterol; INR-PT, international normalized ratio of prothrombine time. [a]*n* = 23 for women, 13 for men. [b]*n* = 22 for women, 13 for men. [c]*n* = 21 for women, 12 for men.

active in liver and altered following exposure to glucolipotoxic (high glucose and lipid) conditions. To test this, we first measured mRNA expression of IL-6 trans-signaling components in human hepatocyte (HepG2), quiescent or activated hepatic stellate (LX-2), and unactivated or activated macrophage (THP-1) cell lines to determine the source(s) of these proteins. Although all cell types expressed transcripts for *IL-6*, *IL-6Rα*, and *GP130*, LX-2 stellate cells expressed significantly higher *IL-6* (Supplementary Fig. 1*A*) and *GP130* mRNA (Supplementary Fig. 1*C*) compared with other cell types. Only HepG2 hepatocytes and THP-1 macrophage cells expressed appreciable levels of IL-6 receptor (*IL-6R*) transcripts (Supplementary Fig. 1*B*).

Although all cell lines expressed *IL-6* mRNA, only LX-2 stellate cells secreted IL-6 (Fig. 1*A*). In line with our expression data, only HepG2 hepatocytes and THP-1 immune cells secreted the soluble sIL-6R (Fig. 1*E* and *H*), confirming observations by Lemmers et al. (11). We also found that HepG2

Table 2—Anthropometric, metabolic, and clinical characteristics of patients with class 3 obesity

	Total (*n* = 245)	Women (*n* = 122)	Men (*n* = 123)	*P*
Baseline characteristics				
Weight (kg)	135.8 ± 26.4	126.0 ± 22.1	145.5 ± 26.8	**<0.0001**
Height (cm)	168.1 ± 9.3	161.5 ± 6.5	174.6 ± 6.7	**<0.0001**
Age (years)	45.2 ± 11.4	44.0 ± 11.1	46.4 ± 11.6	0.099
BMI (kg/m^2)	47.9 ± 7.8	48.2 ± 7.5	47.7 ± 8.2	0.234
Clinical parameters, *n* (%)				
Diabetes	99 (40.4)	58 (47.5)	41 (33.3)	**0.023**
Bedossa algorithm for NASH, *n* (%)				
No NAFLD	4 (1.6)	4 (3.3)	0 (0.0)	**0.042**
NAFLD	199 (81.9)	95 (78.5)	104 (85.2)	
NASH	40 (16.5)	22 (18.2)	18 (14.8)	
Medications, *n* (%)				
Hypertension	111 (45.3)	44.0 (36.1)	67.0 (54.5)	**0.004**
Metformin	37 (15.1)	19.0 (15.6)	18.0 (14.6)	0.837
Other medication for diabetes	30 (12.2)	13.0 (10.7)	17.0 (13.8)	0.450
Dyslipidemia	54 (22.0)	23.0 (18.9)	31.0 (25.2)	0.231
Biochemical parameters				
Glycemia (mmol/L)	6.4 ± 2.0	6.6 ± 2.3	6.2 ± 1.6	0.316
HbA_{1c} (%)[a]	6.0 ± 1.3	6.1 ± 1.1	6.0 ± 1.1	0.625
Cholesterol (mmol/L)	4.5 ± 1.0	4.6 ± 0.9	4.5 ± 1.0	0.572
HDL (mmol/L)	1.2 ± 0.4	1.3 ± 0.3	1.1 ± 0.5	**<0.0001**
LDL (mmol/L)[b]	2.6 ± 0.9	2.6 ± 0.8	2.6 ± 0.9	0.992
Triglyceride (mmol/L)	1.7 ± 0.8	1.5 ± 0.6	1.9 ± 1.0	**0.042**
ALT (IU/L)	33.9 ± 22.4	33.4 ± 28.6	34.4 ± 14.0	**0.002**
Plasma levels of cytokines				
IL-6 (pg/mL)	8.1 ± 16.5	10.5 ± 22.7	5.8 ± 4.3	**<0.0001**
sIL-6R (ng/mL)	42.0 ± 9.3	42.6 ± 9.3	41.5 ± 9.3	0.335
sgp130 (ng/mL)	316.3 ± 54.9	317.1 ± 55.5	315.4 ± 54.6	0.807

Data are means ± SD for continuous data and sample size (*n*) and percent within the population (%) for categorical data. *P* value shows comparisons between men and women, measured with unpaired *t* test for continuous data and χ^2 or Fisher exact test for categorical data. Bolded *P* values represent statistically significant differences. [a]*n* = 122 for women, 120 for men. [b]*n* = 122 for women, 121 for men.

and LX-2 cells secreted 10-fold more sgp130 than THP-1 cells (Fig. 1*C*, *F*, and *I*). Activation of the stellate cell line with transforming growth factor-β did not impact IL-6 or sgp130 secretion (Fig. 1*A* and *C*), while activation of THP-1 monocytes with PMA decreased sIL-6R and sgp130 secretion (Fig. 1*H* and *I*). Wolf et al. (22), also reported decreased sgp130, but not sIL-6R secretion, following macrophage activation. These results show that the liver can be a source of IL-6 trans-signaling mediators; however, a coordinated response from multiple hepatic cell types is required for secretion of all components of the soluble complex.

NAFLD is related to and influenced by metabolic disorders associated with hyperglycemia and hyperlipidemia, including diabetes, obesity, and cardiovascular disease (23). For exploration of whether glucolipotoxicity influences secretion of IL-6 trans-signaling mediators, cell lines were exposed to high glucose and lipid. LX-2 stellate cells secreted more sgp130 when cultured in glucolipotoxic conditions (regardless of state), while significant increases in IL-6 secretion did not occur unless cells were activated (Fig. 1*A* and *C*). High glucose and palmitate did not change secretion patterns from HepG2 or THP-1 cells (Fig. 1*D–I*). These results suggest that glucolipotoxicity may impact secretion of IL-6 trans-signaling mediators from hepatic stellate cells.

sgp130 levels can be regulated by expression or proteolytic cleavage of gp130 on the plasma membrane (22). For determination of how glucolipotoxicity leads to increased spg130 secretion, LX-2 cells were treated with GI (ADAM10 inhibitor) or GW (ADAM10/17 inhibitor) prior to and during glucolipotoxic challenge. GI and GW similarly inhibited high glucose– and lipid-induced sgp130 secretion (Fig. 2*A*), suggesting ADAM10 as a potential protease implicated in cleavage of gp130. Consistent with proteolysis underlying sgp130 secretion, the mature, activated form of ADAM10 (mADAM10) was increased in response to high glucose and lipids (Fig. 2*B*) and this was inhibited by GI and GW without any changes in *ADAM10* mRNA (Supplementary Fig. 1*D*) or total proenzyme levels (proADAM10) (Fig. 2*B*). These results suggest that glucolipotoxicity activates ADAM10, which promotes secretion of sgp130 from stellate cells.

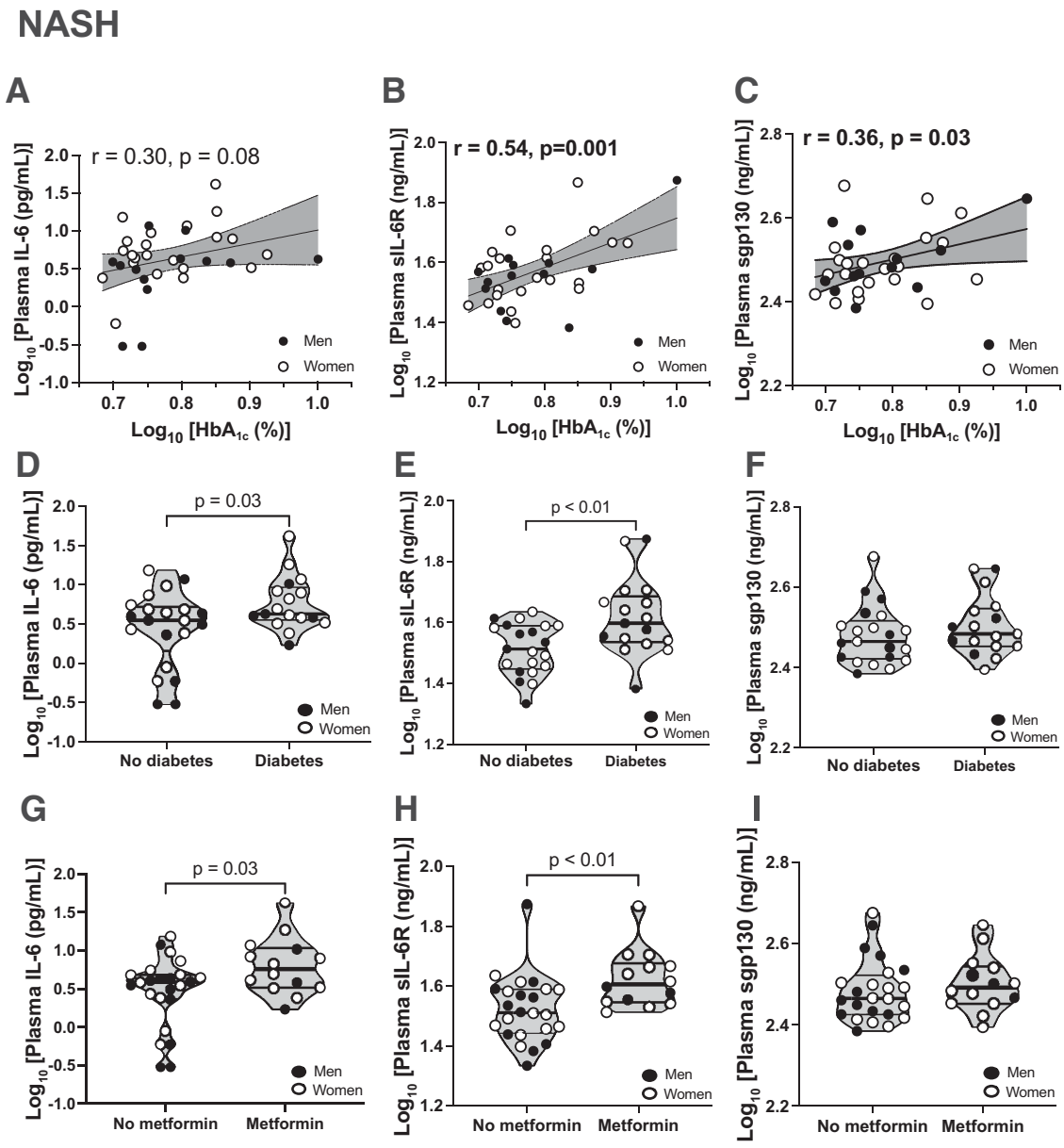

Figure 3—IL-6 trans-signaling correlates with HbA_{1c}, diabetes, and metformin use in NASH. Pearson correlations between plasma IL-6 (*A*), sIL-6R (*B*), and sgp130 (*C*) with plasma HbA_{1c} in patients with NASH. n = 22 women and n = 13 men. Plasma concentrations of IL-6, sIL-6R, and sgp130 in patients with NASH compared among patients with diabetes (*D–F*) and metformin use (*G–I*). Analysis was conducted with *t* test; n = 24 women, n = 14 men.

Circulating IL-6 Trans-Signaling Mediators Are Increased in Diabetes and Associated With Blood Glucose in Subjects With NAFLD and NASH

Since glucolipotoxicity altered secretion of IL-6 and sgp130 from hepatic stellate cells, we investigated whether circulating levels of IL-6 trans-signaling proteins are altered in NAFLD and whether this is impacted by diabetes. To this end, we measured plasma levels from subjects with biopsy-confirmed NAFLD or NASH from two patient biobanks. The first cohort was comprised of subjects with NASH with MRI/MRE assessment of liver disease concurrent with blood sampling (n = 38) (Table 1). Among this population, 100% had NASH, 44.7% subjects had diabetes, 47.4% had obesity, 31.6% had hyperlipidemia, and 36.8% were taking metformin. The second cohort was comprised of subjects with class 3 obesity, for whom blood and liver tissue were collected at the time of bariatric surgery (Table 2). In this population, 100% were obese, 81.9% had NAFLD, 16.5% had NASH based on Bedossa scoring (20), 40.4% had diabetes, and 15.1% were taking metformin. Consistent with diabetes being a risk factor for advanced liver disease, people with NAFLD/NASH and diabetes had higher steatosis grade, activity score, and fibrosis stage than those without diabetes (Supplementary Fig. 2*A–F*).

In healthy subjects, normal plasma levels of IL-6 are <3 pg/mL (24,25) and average plasma concentrations of

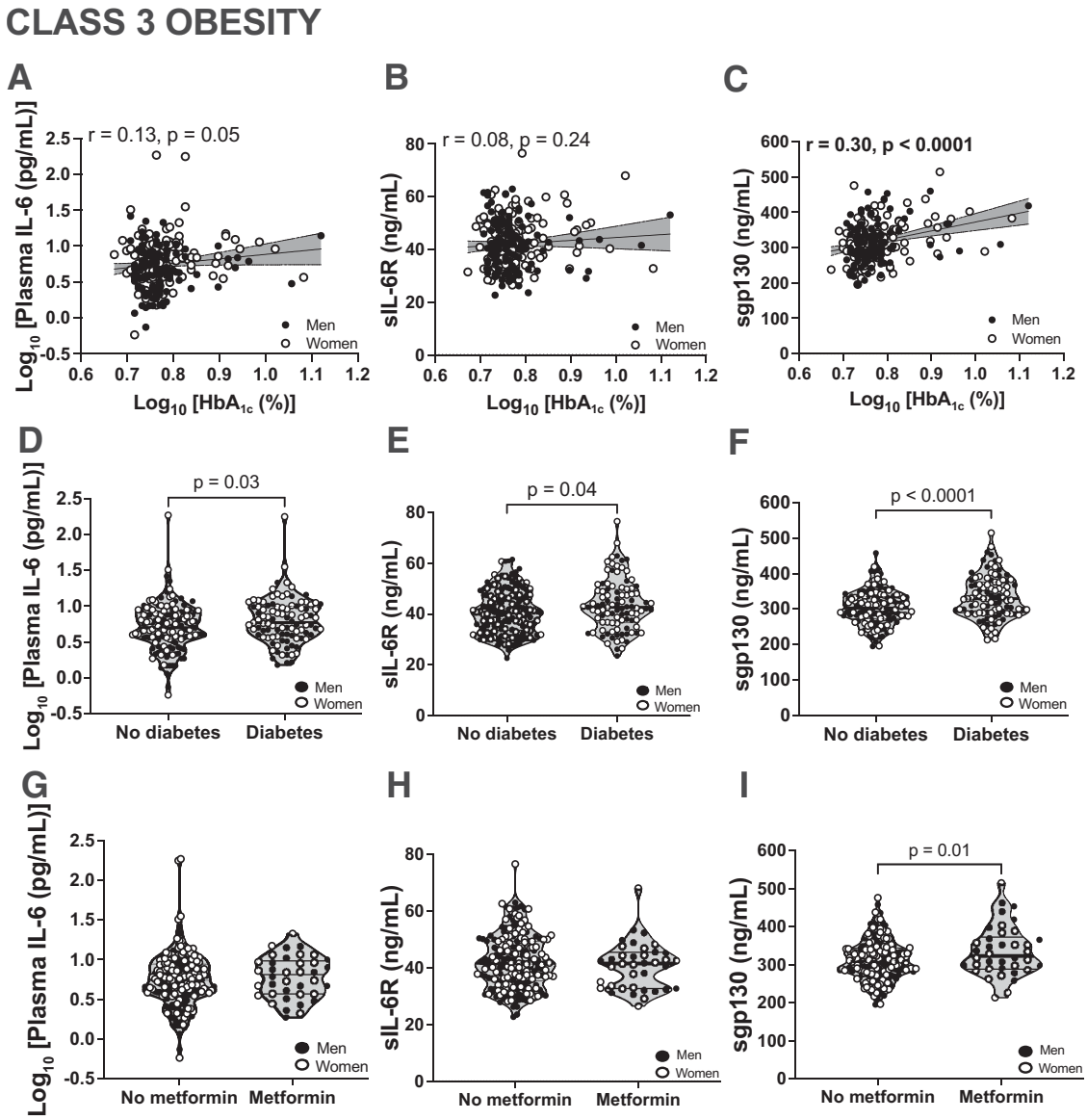

Figure 4—IL-6 trans-signaling correlates with HbA_{1c}, diabetes, and metformin use in class 3 obesity. Pearson correlations between plasma IL-6 (*A*), sIL-6R (*B*), and sgp130 (*C*) and plasma HbA_{1c} in patients with class 3 obesity. n = 122 women, n = 120 men. Plasma concentrations of IL-6, sIL-6R, and sgp130 in patients with class 3 obesity compared among patients with diabetes (*D–F*) and metformin use (*G–I*). Analysis was conducted with t test; n = 122 women, n = 123 men.

sIL-6R and sgp130 are 35 ng/mL and 217 ng/mL, respectively (25,26). In our NASH cohort, average plasma IL-6 and sgp130 levels were above normal at 6.1 pg/mL and 313.8 ng/mL, respectively, while average levels of sIL-6R were within normal range (37.7 ng/mL) (Table 1). In the class 3 obesity cohort, average plasma IL-6, sIL-6R, and sgp130 were all above levels in healthy subjects (25,26) (8.1 pg/mL, 42.0 ng/mL, and 316.3 ng/mL, respectively) (Table 2). We also noted that circulating IL-6 was higher in women, sIL-6R and sgp130 were influenced by age, and there was a significant positive correlation between BMI and circulating IL-6 or sIL-6R (Supplementary Figs. 3 and 4), in line with previously published findings (27,28).

Given the close relationship between glucotoxicity and NAFLD severity (29), we first investigated whether IL-6 trans-signaling mediators varied with blood lipids or glycated hemoglobin (HbA_{1c}). We found no consistent relationships between plasma cholesterol or triglycerides with any component of the circulating IL-6 trans-signaling complex (Supplementary Fig. 5). However, in the NASH cohort we observed clear correlations between HbA_{1c} and sIL-6R or sgp130 (Fig. 3*B* and *C*) and HbA_{1c} with sgp130 in the class 3 obesity cohort (Fig. 4*C*). Consistently, plasma IL-6 and sIL-6R in the NASH cohort (Fig. 3*D* and *E*), and all three trans-signaling components in the obese population, were significantly higher in subjects with NASH and concurrent diabetes (Fig. 4*D–F*). Metformin can reduce inflammatory signaling (30); yet, IL-6 and sIL-6R were higher in individuals with NASH taking metformin (Fig. 3*G* and *H*) and sgp130 was

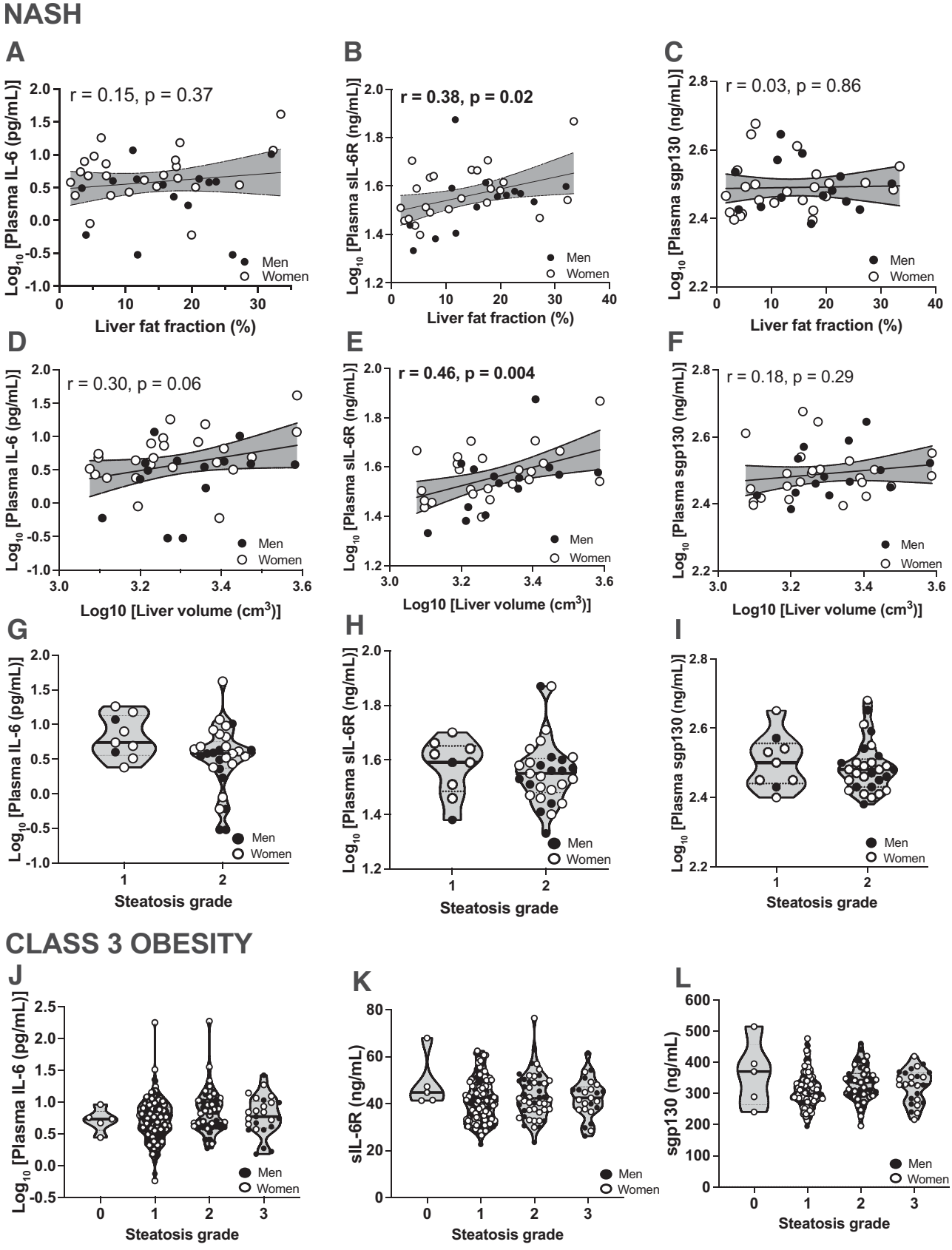

Figure 5—Plasma sIL-6R correlates with hepatic fat content and volume by imaging but not steatosis grade. Pearson correlations between plasma IL-6 (*A* and *D*), sIL-6R (*B* and *E*), and sgp130 (*C* and *F*) and MRE/MRI measures of liver fat fraction and liver volume in patients with NASH. n = 24 women and n = 14 men. Plasma concentrations of IL-6 (*G* and *J*), sIL-6R (*H* and *K*), and sgp130 (*I* and *L*) in

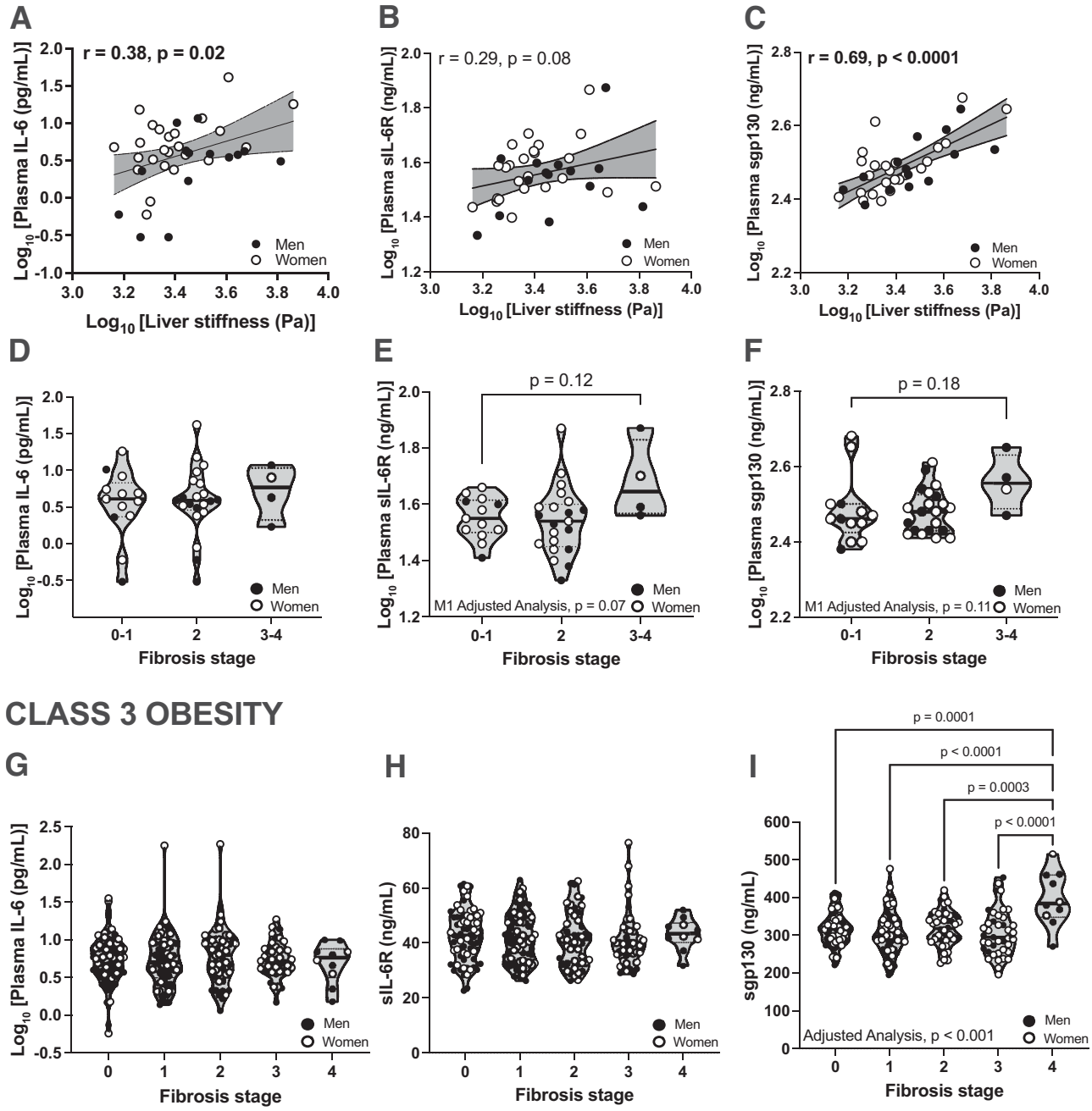

Figure 6—sgp130 correlations with liver stiffness and fibrosis in people with NAFLD/NASH. Pearson correlations between plasma IL-6 (*A*), sIL-6R (*B*), and sgp130 (*C*) and MRE/MRI measures of liver stiffness in patients with NASH. n = 24 women and n = 14 men. Plasma concentrations of IL-6 (*D* and *G*), sIL-6R (*E* and *H*), and sgp130 (*F* and *I*) in patients with NASH and class 3 obesity compared among liver biopsy measures of fibrosis stage. Data presented for subjects with NASH with fibrosis stage F0 (n = 1, pooled with F1), F1 (n = 12), F2 (n = 21), F3 (n = 3), and F4 (n = 1, pooled with F3) and class 3 obesity stage F0 (n = 73), F1 (n = 73), F2 (n = 48), F3 (n = 41), and F4 (n = 10). Analysis was conducted with one-way ANOVA with multiple comparisons with adjustment for age, sex, BMI, and diabetes and metformin use.

higher in individuals with obesity taking metformin (Fig. 4*I*). Interestingly, the relationship between sIL-6R and HbA_{1c} was not seen in the obesity cohort (Fig. 4*B*). This may be explained by sex differences, as we found significant associations between sIL-6R and HbA_{1c} in women of both cohorts (NASH, r = 0.39, P = 0.02; class 3 obesity, r = 0.17, P = 0.06) but not men

patients with NASH and class 3 obesity compared among liver biopsy measures of steatosis grade. Data presented for subjects with NASH with steatosis grade G1 (n = 9) and G2 (n = 29) and class 3 obesity grade G0 (n = 5), G1 (n = 168), G2 (n = 47), and G3 (n = 25). Analysis was conducted with one-way ANOVA with multiple comparisons with adjustment for age, sex, BMI, and diabetes or metformin use.

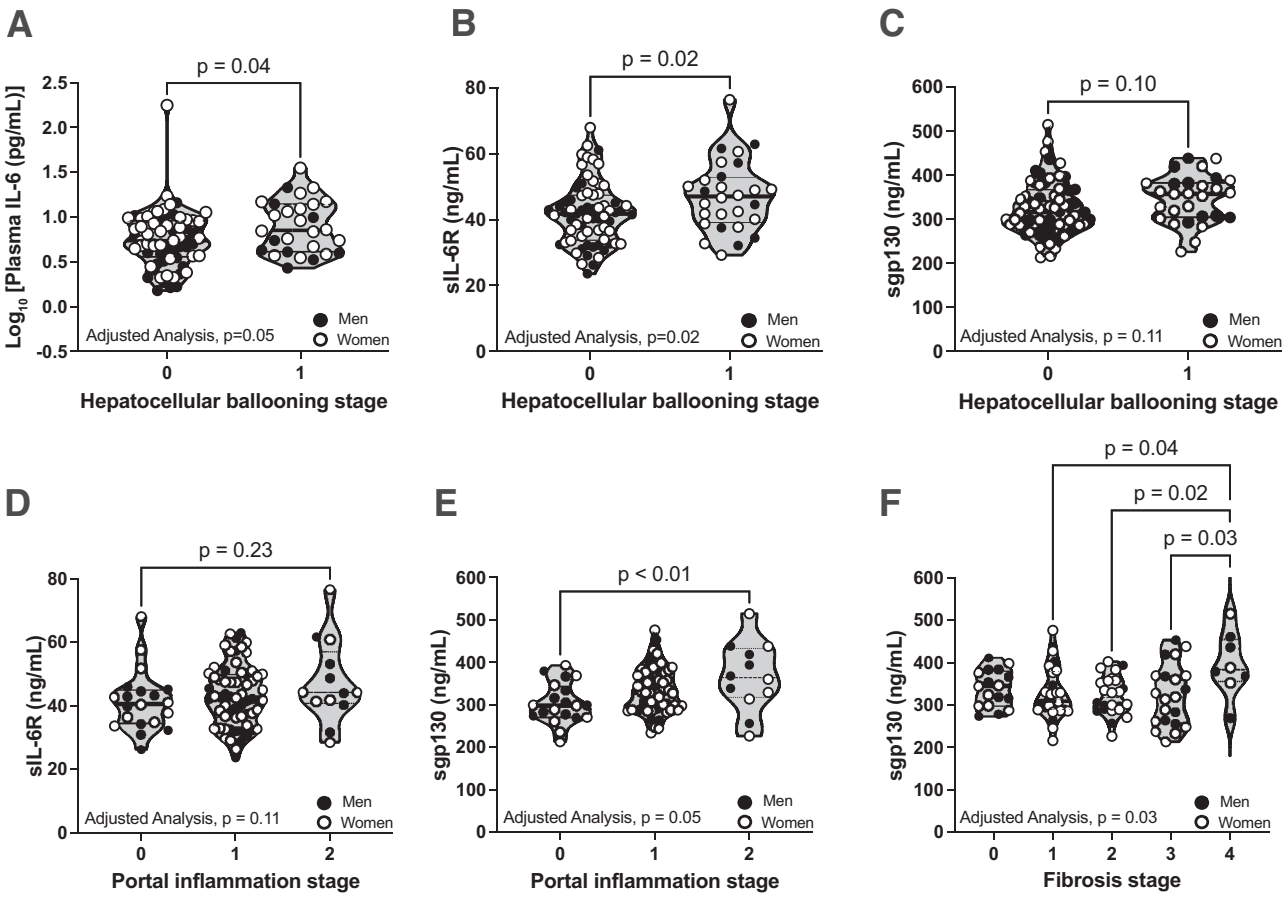

Figure 7— Increased IL-6 trans-signaling is associated with histological markers of liver inflammation in obese patients with NAFLD and concurrent diabetes. Plasma concentrations of IL-6, sIL-6R, or sgp130 in patients with class 3 obesity and diabetes compared with measures of hepatocellular ballooning stage (*A–C*) and liver portal inflammation (*D* and *E*) and fibrosis (*F*) stage determined with histology. Data presented for subjects with hepatocellular ballooning stage S0 (n = 69) and S1 (n = 28); subjects with portal inflammation stage S0 (n = 20), S1 (n = 64), S2 (n = 11), and S3 (n = 2, pooled with S2); and subjects with fibrosis stage S0 (n = 17), S1 (n = 29), S2 (n = 24), S3 (n = 21), and S4 (n = 8). Analysis was conducted with one-way ANOVA with multiple comparisons with adjustment for age, sex, BMI, and diabetes and metformin use.

(NASH, r = 0.01, P = 0.97; class 3 obesity, r = 0.04, P = 0.70). Taken together with in vitro data, our data suggest a strong association between circulating regulators of IL-6 trans-signaling and diabetes that may be associated with increased secretion within a setting of hyperglycemia.

Circulating IL-6 Signaling Mediators Correlate With NAFLD Pathology

We next sought to determine whether circulating levels of IL-6 trans-signaling mediators were associated with pathological features of fatty liver disease, including hepatic lipid content, inflammation, and/or fibrosis. In both human cohorts, liver disease severity was determined with biopsy samples, while in the NASH cohort we also had access to data from MRI/MRE scans. Liver volume and stiffness measured with MRI/MRE have good prognostic value to predict liver disease severity (31–34), with much greater surface area covered than with biopsy alone.

Plasma sIL-6R positively correlated with liver fat fraction (Fig. 5*B*) and liver volume (Fig. 5*E*) in the NASH cohort. However, stepwise forward regression analysis adjusted with model 1 (Supplementary Table 1) or 2 (Supplementary Table 2) demonstrated that these correlations may be influenced by BMI or metformin. Given strong relationships between BMI and liver fat/volume (35) and BMI and sIL-6R (Supplementary Fig. 3), it is impossible to delineate the contribution of liver fat versus whole-body adiposity. However, we did not observe a significant relationship between steatosis grade in biopsies and any circulating proteins in either cohort (Fig. 5*J–L*). Overall, data suggest that sIL-6R correlates with adiposity, but further exploration is needed to determine whether this is directly related to hepatic fat.

Plasma sgp130 Correlates With Advanced Liver Disease in NASH and Class 3 Obesity

Given our observation that high glucose and lipids stimulated sgp130 secretion from stellate cells, we next evaluated

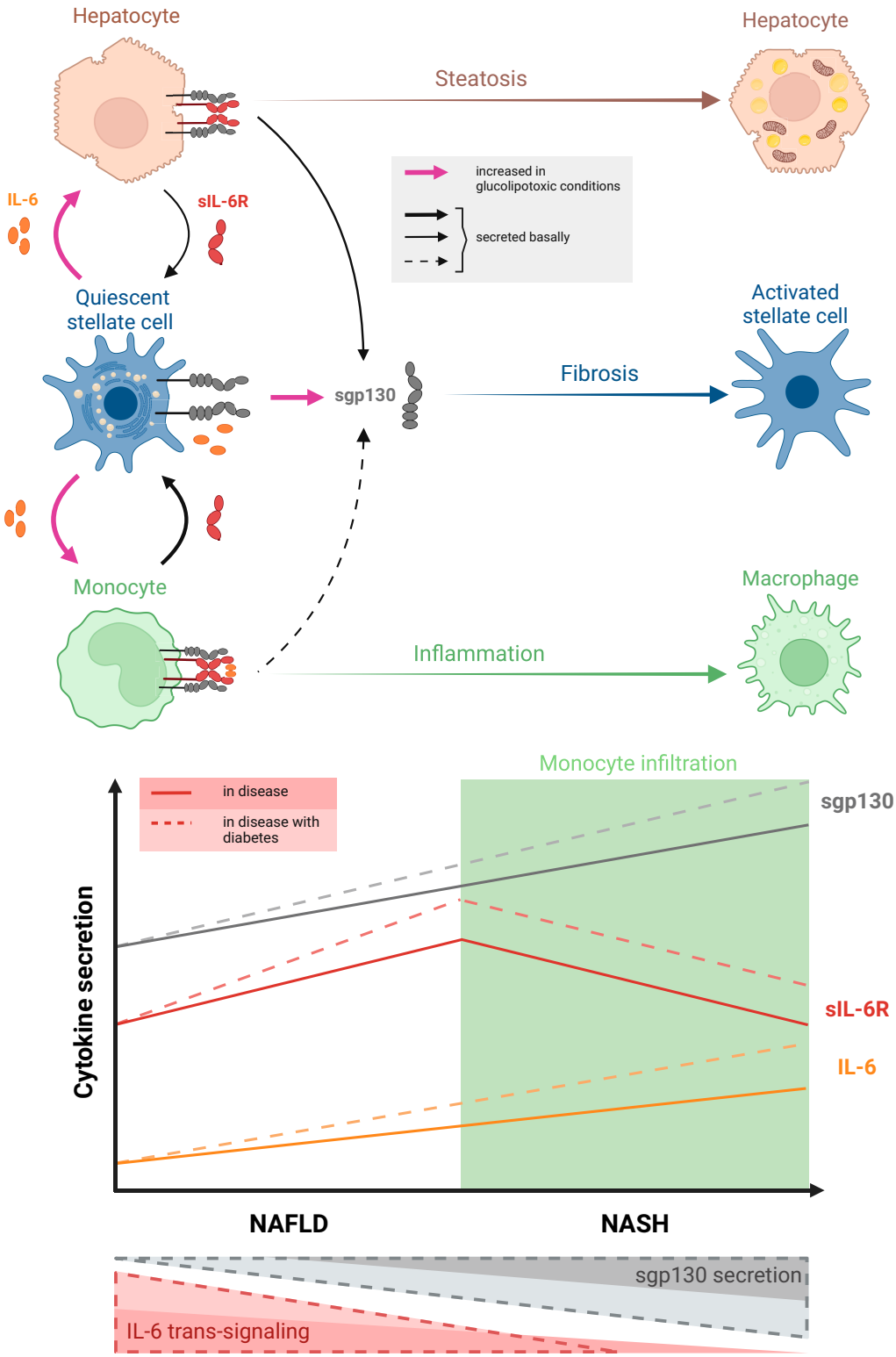

Figure 8—IL-6 trans-signaling mediator secretion is controlled by different liver cell types in their microenvironment. Hepatocytes and monocytes secrete sIL-6R basally, which can induce IL-6 trans-signaling in quiescent hepatic stellate cells. In return, hepatic stellate cells secrete sgp130, blunting IL-6 trans-signaling and facilitating classical signaling in hepatocytes and monocytes. Progression of NAFLD, which promotes monocyte infiltration in liver and activation into macrophages, could result in lower levels of sIL-6R from macrophages and higher amounts of sgp130 from stellate cells. In this context, inhibition of IL-6 trans-signaling in liver might be linked to steatotic hepatocytes, hepatic stellate cell activation and fibrosis, and chronic liver inflammation. In diabetes, the secretion of IL-6, sIL-6R, and sgp130 is significantly increased, which could exacerbate this pathway to accelerate the disease. The scheme was created with BioRender (biorender.com).

relationships between circulating IL-6 trans-signaling components and liver fibrosis. Both plasma IL-6 and plasma sgp130 positively correlated with liver stiffness (Fig. 6*A* and *C*) in the NASH cohort, with plasma sgp130 showing a particularly strong linear association ($r = 0.69$, $P < 0.0001$). When adjustment with model 1 or model 2, our results show that plasma sgp130 level correlated with liver stiffness independent of all covariates (Supplementary Tables 1 and 2). We also noted a trend toward higher sIL-6R and sgp130 in NASH patients with advanced fibrosis stage versus F0–F1 (Fig. 6*E* and *F*) (sIL-6R, adjustment with model 1, $P = 0.07$, and model 2, $P = 0.05$; sgp130, adjustment with model 1, $P = 0.11$, and model 2, $P = 0.12$), while only plasma sgp130 was significantly higher in obese subjects with F4 fibrosis compared with all other stages (Fig. 6*I*) (adjustment with age, sex, BMI, diabetes, and metformin; $P < 0.001$). Taken together, data from both cohorts suggest that increased circulating sgp130 can indicate liver fibrosis in NAFLD.

Liver stiffness (measured with MRI/MRE) is highly related to fibrosis but also influenced by inflammation and steatosis (36). Activity score is a composite value of indices given for histological evidence of inflammation (lobular and/or portal) and hepatocyte ballooning (an indication of hepatocyte damage). Plasma IL-6, sIL-6, and sgp130 did not correspond with activity score in either cohort (Supplementary Fig. 6*A*–*F*). Hepatocyte ballooning trended higher with increased plasma IL-6, and portal inflammation trended higher with increased plasma sIL-6R (Supplementary Fig. 6*G* and *L*). No associations were noted with lobular inflammation. Since metabolic inflammation is intimately linked to diabetes, we investigated whether diabetes influenced these associations. Interestingly, when considering only subjects with both NAFLD and diabetes, all IL-6 trans-signaling components were associated with hepatocyte ballooning (Fig. 7*A*–*C*) and sgp130 was significantly associated with increased portal inflammation and fibrosis (Fig. 7*E* and *F*). Thus, diabetes accentuated associations of IL-6 and sgp130 with liver pathology in NAFLD, suggesting that enhanced IL-6 trans-signaling in diabetes may exacerbate NASH.

DISCUSSION

In this study we explored relationships among three components of the IL-6 signaling pathway (IL-6, sIL-6R, and sgp130), diabetes, and steatotic liver disease. We provide novel data showing that in people with NAFLD, diabetes and hyperglycemia are associated with higher plasma concentrations of IL-6 trans-signaling mediators. Our data in cell lines suggest that high blood glucose and lipids promote ADAM10 activation and proteolytic cleavage of gp130, potentiating sgp130 secretion from hepatic stellate cells along with IL-6 (Fig. 8). In line with IL-6 trans-signaling playing a role in NAFLD pathobiology, higher plasma sgp130 strongly correlated with liver stiffness and was associated with histological evidence of liver fibrosis. IL-6 trans-signaling was also associated with liver inflammation in people with concurrent diabetes.

Higher IL-6 is often observed in metabolic disease (5,12–14,37–39), but much less is known about its circulating coreceptors or how their secretion is regulated. Our data support the liver as a possible source for the circulating components of IL-6 trans-signaling in NAFLD (sIL-6R and sgp130). Most notably, all three circulating IL-6 trans-signaling components were further increased in concomitant diabetes. We show that different liver cell types secrete components of the complex and their secretion is influenced by high glucose and lipids, and we report higher circulating IL-6 and sgp130 in NAFLD/NASH aligning with increases seen in alcoholic steatotic liver disease (11). Circulating sIL-6R in both our cohorts were within normal ranges (25), while in a previous study investigators found increased plasma sIL-6R in NASH (40). However, we did not include healthy subjects for direct comparison.

There are close relationships between hyperglycemia and chronic liver disease. High blood glucose positively correlates with hepatic insulin resistance, which can result in excessive fat accumulation. Elevated blood glucose can also amplify oxidative stress and trigger secretion of inflammatory cytokines, creating a state of low but constitutive inflammation that damages liver cells and plays a critical role in development of liver fibrosis (41). Our data showing a relationship between circulating IL-6 coreceptors and HbA_{1c}, together with in vitro data linking increased sgp130 secretion from stellate cells in response to glucolipotoxicity, lead us to propose that IL-6 trans-signaling plays a direct role in the unique pathogenesis of NAFLD associated with diabetes.

The physiological role of IL-6 trans-signaling within liver is controversial. Total ablation of hepatic IL-6 signaling in mice causes steatosis and fibrosis (40), but this does not discriminate between classical- and trans-signaling. Activation of both classical and trans IL-6 signaling is associated with increased cellular proliferation via STAT3, but trans-signaling seems to prolong activation (42). Blockade of IL-6 trans-signaling with sgp130 decreases liver regeneration following partial hepatectomy (43), while activation of IL-6 trans-signaling promotes regeneration (44,45) and aggravates liver cancer in mice (46,47). In our study, the strong correlation between sgp130 and liver stiffness/fibrosis suggests that increased IL-6 trans-signaling (IL-6 and sIL-6R) might promote repair in response to liver damage or inflammation. Since sgp130 acts as a natural inhibitor for IL-6 trans-signaling, higher secretion (i.e., by glucolipotoxicity) could inhibit repair and promote NASH progression. However, our ability to draw mechanistic links is limited by the correlative nature of human data; thus, further investigation is needed to determine whether decreased local IL-6 trans-signaling could be responsible for worsening inflammation and/or fibrosis in NAFLD.

Limitations of our study include use of isolated, immortalized cell lines and lack of an in vivo model. It is difficult to target IL-6 alone, differentiate classical versus trans-signaling, or isolate tissue-specific roles using available mouse models. Interestingly, transgenic overexpression of human sgp130 in

mice does not exacerbate diet-induced NAFLD (48,49), but chronic increases may promote obesity and fatty liver with age (50), suggesting that decreased trans-signaling could potentiate metabolic disease.

One interesting possibility stemming from our data is that plasma sgp130 (alone or in combination with sIL-6R) might be an effective, noninvasive method to predict the severity of liver disease in NASH. We present this as a hypothesis-generating observation and recognize that a larger sample size and additional analysis are required to test whether IL-6 trans-signaling proteins are biomarkers of NAFLD/NASH. Yet, we found it interesting that while sgp130 correlates very well with liver stiffness by MRI/MRE, its correlation with the stage of histological fibrosis was less pronounced. Liver fibrosis in biopsies is scored based on collagen staining, while MRE-determined liver stiffness is influenced by fibrosis, inflammation, and steatosis (32–34). sgp130 is a component of an inflammatory pathway, which could explain its stronger correlation with liver stiffness versus collagen (a late consequence of damage). Our data may also suggest that high sgp130 represents active NASH (i.e., inflammatory state) instead of collagen deposition (fibrosis).

In conclusion, our data support that circulating components of the IL-6 trans-signaling system correlate with NAFLD/NASH pathogenesis and that liver may be a source of these mediators in metabolic disease. Our data also suggest a link between diabetes and/or hyperglycemia and hepatic IL-6 trans-signaling. Strong associations of IL-6, sIL-6R, and sgp130 with liver pathobiology imply that these circulating proteins may be locally involved in NAFLD pathogenesis and suggest further investigation into whether higher plasma levels indicate liver damage, particularly in people with concurrent NAFLD and diabetes.

Acknowledgments. The authors acknowledge the invaluable collaboration of the surgery team, bariatric surgeons, and biobank staff of the IUCPQ. The authors also thank Paule Bodson Clermont, Centre de Recherche du Centre Hospitalier de l'Université de Montréal (CRCHUM), Hannah Zhang, Institut de recherches cliniques de Montréal (IRCM), Mélissa Léveillé (IRCM) and Stewart Jeromson (IRCM) for their assistance.

Patients and the public were not involved in the design, conduct, reporting, or dissemination plans of the authors' research.

Funding and Duality of Interest. This work was supported by unrestricted operating grants from Merck Sharp & Dohme/University of Montreal and the International Development Research Centre (108591-001). J.L.E. and A.T. are supported by Chercheurs-boursiers Senior awards from Fonds de recherche du Québec Santé. The IUCPQ Biobank is supported by the IUCPQ Foundation and Research Center. L.B. receives funding from Johnson & Johnson, Medtronic, Bodynov, and GI Windows for studies on bariatric surgery. A.T. and J.L.E. received a speaking honorarium from Eli Lilly. No other potential conflicts of interest relevant to this article were reported.

Author Contributions. A.T. and J.L.E. designed studies. C.H. and A.B. managed the NASH clinical study. L.Bie. and A.L. designed and carried out the bariatric surgery study. A.G., C.S., L.Bil., C.Ba., and A.T. acquired, analyzed, and interpreted data. M.F. assisted with data analysis. B.N.N. scored histological samples. L.Bil., A.C., E.G., C.Bé., M.B., J.-M.G., M.L., A.T., M.F., and J.L.E. contributed intellectual content toward study design and interpretation. C.Y.C. scored liver histological samples. A.G., C.S., M.F., and J.L.E. wrote the manuscript. All authors reviewed the manuscript. J.L.E. is the guarantor of this work and, as such, had full access to all the data in the study and takes responsibility for the integrity of the data and the accuracy of the data analysis.

Prior Presentation. Parts of this study were presented in abstract form at the 2022 Canadian Liver Meeting, Ottawa, Ontario, Canada, 12–15 May 2022; IRCM 2022 Scientific Forum, Orford, Quebec, Canada, 2–3 June 2022; International Liver Congress 2022, London, U.K., 22–26 June 2022; XVIIIth Scientific Day of Molecular Biology Programs, Montreal, QC, Canada, 5 May 2023; and IRCM 2023 Scientific Forum, Carlin, British Columbia, Canada, 8–9 June 2023.

References

1. Younossi ZM, Koenig AB, Abdelatif D, Fazel Y, Henry L, Wymer M. Global epidemiology of nonalcoholic fatty liver disease-meta-analytic assessment of prevalence, incidence, and outcomes. Hepatology 2016;64:73–84

2. Huang DQ, El-Serag HB, Loomba R. Global epidemiology of NAFLD-related HCC: trends, predictions, risk factors and prevention. Nat Rev Gastroenterol Hepatol 2021;18:223–238

3. Rinella ME, Lazarus JV, Ratziu V, et al.; NAFLD Nomenclature consensus group. A multi-society Delphi consensus statement on new fatty liver disease nomenclature. Hepatology. 24 June 2023 [Epub ahead of print]. DOI: 10.1097/HEP.0000000000000520

4. Cuthbertson DJ, Koskinen J, Brown E, et al. Fatty liver index predicts incident risk of prediabetes, type 2 diabetes and non-alcoholic fatty liver disease (NAFLD). Ann Med 2021;53:1256–1264

5. Yeste D, Vendrell J, Tomasini R, et al. Interleukin-6 in obese children and adolescents with and without glucose intolerance. Diabetes Care 2007;30:1892–1894

6. Charles BA, Doumatey A, Huang H, et al. The roles of IL-6, IL-10, and IL-1RA in obesity and insulin resistance in African-Americans. J Clin Endocrinol Metab 2011;96:E2018–E2022

7. Wieckowska A, Papouchado BG, Li Z, Lopez R, Zein NN, Feldstein AE. Increased hepatic and circulating interleukin-6 levels in human nonalcoholic steatohepatitis. Am J Gastroenterol 2008;103:1372–1379

8. Giraldez MD, Carneros D, Garbers C, et al. New insights into IL-6 family cytokines in metabolism, hepatology and gastroenterology. Nat Rev Gastroenterol Hepatol 2021;18:787–803

9. Schmidt-Arras D, Rose-John S. IL-6 pathway in the liver: from physiopathology to therapy. J Hepatol 2016;64:1403–1415

10. Uhlén M, Fagerberg L, Hallström BM, et al. Proteomics. Tissue-based map of the human proteome. Science 2015;347:1260419

11. Lemmers A, Gustot T, Durnez A, et al. An inhibitor of interleukin-6 trans-signalling, sgp130, contributes to impaired acute phase response in human chronic liver disease. Clin Exp Immunol 2009;156:518–527

12. Weiss TW, Arnesen H, Seljeflot I. Components of the interleukin-6 transsignalling system are associated with the metabolic syndrome, endothelial dysfunction and arterial stiffness. Metabolism 2013;62:1008–1013

13. Nikolajuk A, Kowalska I, Karczewska-Kupczewska M, et al. Serum soluble glycoprotein 130 concentration is inversely related to insulin sensitivity in women with polycystic ovary syndrome. Diabetes 2010;59:1026–1029

14. Chen H, Zhang X, Liao N, Wen F. Increased levels of IL-6, sIL-6R, and sgp130 in the aqueous humor and serum of patients with diabetic retinopathy. Mol Vis 2016;22:1005–1014

15. Venkatesh SK, Yin M, Ehman RL. Magnetic resonance elastography of liver: technique, analysis, and clinical applications. J Magn Reson Imaging 2013;37:544–555

16. Hines CD, Bley TA, Lindstrom MJ, Reeder SB. Repeatability of magnetic resonance elastography for quantification of hepatic stiffness. J Magn Reson Imaging 2010;31:725–731

17. Tang A, Dzyubak B, Yin M, et al. MR elastography in nonalcoholic fatty liver disease: inter-center and inter-analysis-method measurement reproducibility and accuracy at 3T. Eur Radiol 2022;32:2937–2948

18. Kleiner DE, Brunt EM, Van Natta M, et al.; Nonalcoholic Steatohepatitis Clinical Research Network. Design and validation of a histological scoring system for nonalcoholic fatty liver disease. Hepatology 2005;41:1313–1321
19. Brunt EM, Janney CG, Di Bisceglie AM, Neuschwander-Tetri BA, Bacon BR. Nonalcoholic steatohepatitis: a proposal for grading and staging the histological lesions. Am J Gastroenterol 1999;94:2467–2474
20. Bedossa P, Poitou C, Veyrie N, et al. Histopathological algorithm and scoring system for evaluation of liver lesions in morbidly obese patients. Hepatology 2012;56:1751–1759
21. Pantano L, Agyapong G, Shen Y, et al. Molecular characterization and cell type composition deconvolution of fibrosis in NAFLD. Sci Rep 2021;11:18045
22. Wolf J, Waetzig GH, Chalaris A, et al. Different soluble forms of the interleukin-6 family signal transducer gp130 fine-tune the blockade of interleukin-6 trans-signaling. J Biol Chem 2016;291:16186–16196
23. Eslam M, Newsome PN, Sarin SK, et al. A new definition for metabolic dysfunction-associated fatty liver disease: an international expert consensus statement. J Hepatol 2020;73:202–209
24. Reference Values for Biochemical Tests - Centre hospitalier de l'Université de Montréal. Accessed 29 October 2019. Available from https://www.chumontreal.qc.ca/sites/default/files/2022-10/Valeurs%20références%20-%20Biochimie-%202022-10-11%20%281%29.pdf
25. Nikolaus S, Waetzig GH, Butzin S, et al. Evaluation of interleukin-6 and its soluble receptor components sIL-6R and sgp130 as markers of inflammation in inflammatory bowel diseases. Int J Colorectal Dis 2018;33:927–936
26. Padberg F, Feneberg W, Schmidt S, et al. CSF and serum levels of soluble interleukin-6 receptors (sIL-6R and sgp130), but not of interleukin-6 are altered in multiple sclerosis. J Neuroimmunol 1999;99:218–223
27. Sindhu S, Thomas R, Shihab P, et al. Obesity is a positive modulator of IL-6R and IL-6 expression in the subcutaneous adipose tissue: significance for metabolic inflammation. PLoS One 2015;10:e0133494
28. Kuo FC, Huang YH, Lin FH, et al. Circulating soluble IL-6 receptor concentration and visceral adipocyte size are related to insulin resistance in Taiwanese adults with morbid obesity. Metab Syndr Relat Disord 2017;15:187–193
29. Watt GP, De La Cerda I, Pan JJ, et al. Elevated glycated hemoglobin is associated with liver fibrosis, as assessed by elastography, in a population-based study of Mexican Americans. Hepatol Commun 2020;4:1793–1801
30. Bharath LP, Nikolajczyk BS. The intersection of metformin and inflammation. Am J Physiol Cell Physiol 2021;320:C873–C879
31. Tang A, Cloutier G, Szeverenyi NM, Sirlin CB. Ultrasound elastography and MR elastography for assessing liver fibrosis: part 1, principles and techniques. AJR Am J Roentgenol 2015;205:22–32
32. Costa-Silva L, Ferolla SM, Lima AS, Vidigal PVT, Ferrari TCA. MR elastography is effective for the non-invasive evaluation of fibrosis and necroinflammatory activity in patients with nonalcoholic fatty liver disease. Eur J Radiol 2018;98:82–89
33. Chen J, Yin M, Talwalkar JA, et al. Diagnostic performance of MR elastography and vibration-controlled transient elastography in the detection of hepatic fibrosis in patients with severe to morbid obesity. Radiology 2017;283:418–428
34. Park CC, Nguyen P, Hernandez C, et al. Magnetic resonance elastography vs transient elastography in detection of fibrosis and noninvasive measurement of steatosis in patients with biopsy-proven nonalcoholic fatty liver disease. Gastroenterology 2017;152:598–607.e2
35. Loomis AK, Kabadi S, Preiss D, et al. Body mass index and risk of nonalcoholic fatty liver disease: two electronic health record prospective studies. J Clin Endocrinol Metab 2016;101:945–952
36. Lefebvre T, Wartelle-Bladou C, Wong P, et al. Prospective comparison of transient, point shear wave, and magnetic resonance elastography for staging liver fibrosis. Eur Radiol 2019;29:6477–6488
37. Zuliani G, Galvani M, Maggio M, et al. Plasma soluble gp130 levels are increased in older subjects with metabolic syndrome. The role of insulin resistance. Atherosclerosis 2010;213:319–324
38. Bowker N, Shah RL, Sharp SJ, et al. Meta-analysis investigating the role of interleukin-6 mediated inflammation in type 2 diabetes. EBioMedicine 2020;61:103062
39. Skuratovskaia D, Komar A, Vulf M, et al. IL-6 reduces mitochondrial replication, and IL-6 receptors reduce chronic inflammation in NAFLD and type 2 diabetes. Int J Mol Sci 2021;22:1774
40. Hou X, Yin S, Ren R, et al. Myeloid-cell-specific IL-6 signaling promotes microRNA-223-enriched exosome production to attenuate NAFLD-associated fibrosis. Hepatology 2021;74:116–132
41. Targher G, Byrne CD. Clinical review: nonalcoholic fatty liver disease: a novel cardiometabolic risk factor for type 2 diabetes and its complications. J Clin Endocrinol Metab 2013;98:483–495
42. Reeh H, Rudolph N, Billing U, et al. Response to IL-6 trans- and IL-6 classic signalling is determined by the ratio of the IL-6 receptor α to gp130 expression: fusing experimental insights and dynamic modelling. Cell Commun Signal 2019;17:46
43. Fazel Modares N, Polz R, Haghighi F, et al. IL-6 trans-signaling controls liver regeneration after partial hepatectomy. Hepatology 2019;70:2075–2091
44. Galun E, Zeira E, Pappo O, Peters M, Rose-John S. Liver regeneration induced by a designer human IL-6/sIL-6R fusion protein reverses severe hepatocellular injury. FASEB J 2000;14:1979–1987
45. Peters M, Blinn G, Jostock T, et al. Combined interleukin 6 and soluble interleukin 6 receptor accelerates murine liver regeneration. Gastroenterology 2000;119:1663–1671
46. Bergmann J, Müller M, Baumann N, et al. IL-6 trans-signaling is essential for the development of hepatocellular carcinoma in mice. Hepatology 2017;65:89–103
47. Rosenberg N, Van Haele M, Lanton T, et al. Combined hepatocellular-cholangiocarcinoma derives from liver progenitor cells and depends on senescence and IL-6 trans-signaling. J Hepatol 2022;77:1631–1641
48. Kraakman MJ, Kammoun HL, Allen TL, et al. Blocking IL-6 trans-signaling prevents high-fat diet-induced adipose tissue macrophage recruitment but does not improve insulin resistance. Cell Metab 2015;21:403–416
49. Kammoun HL, Allen TL, Henstridge DC, et al. Over-expressing the soluble gp130-Fc does not ameliorate methionine and choline deficient diet-induced non alcoholic steatohepatitis in mice. PLoS One 2017;12:e0179099
50. Lanton T, Levkovitch-Siany O, Udi S, et al. Peripheral sgp130-mediated trans-signaling blockade induces obesity and insulin resistance in mice via PPARα suppression. 24 September 2020 [preprint]. bioRxiv:2020.09.24.309716